Edinburgh Research Explorer

Microfiber Drug/Gene Delivery Platform for Study of Myelination

OPEN ACCESS

1 **Title: Microfiber Drug/Gene Delivery Platform for Study of Myelination**

2 Authors: William Ong[1,2], Junquan Lin[2], Marie E. Bechler[3], Kai Wang[2], Mingfeng Wang[2], Charles

3 ffrench-Constant[3], Sing Yian Chew[2,4*]

4 Affiliations:

1. NTU Institute for Health Technologies (Health Tech NTU), Interdisciplinary Graduate School, Nanyang Technological University, Singapore 637533, Singapore

2. School of Chemical and Biomedical Engineering, Nanyang Technological University, Singapore 637459, Singapore

3. MRC Centre for Regenerative Medicine, The University of Edinburgh, 5 Little France Drive, Edinburgh EH16 4UU, UK

4. Lee Kong Chian School of Medicine, Nanyang Technological University, Singapore 308232, Singapore

* Corresponding author at: School of Chemical and Biomedical Engineering, Nanyang Technological University, Singapore 637459, Singapore.

Tel.: +65 6316 8812; fax: +65 6794 7553

E-mail address: sychew@ntu.edu.sg (S. Y. Chew)

17

1   **Abstract**

2   Our ability to rescue functional deficits after demyelinating diseases or spinal cord injuries is

3   limited by our lack of understanding of the complex remyelination process, which is crucial to

4   functional recovery. In this study, we developed an electrospun suspended poly(ε-caprolactone)

5   microfiber platform to enable the screening of therapeutics for remyelination. As a proof of concept,

6   this platform employed scaffold-mediated non-viral delivery of a microRNA (miR) cocktail to

7   promote oligodendrocyte precursor cells (OPCs) differentiation and myelination. We observed

8   enhanced OPCs differentiation when the cells were transfected with miR-219 and miR-338 on the

9   microfiber substrates. Moreover, miRs promoted the formation of MBP$^+$ tubular extensions around

10   the suspended fibers, which was indicative of myelination, instead of flat myelin membranes on 2D

11   substrates. In addition, OPCs that were transfected with the cocktail of miRs formed significantly

12   longer and larger amounts of MBP$^+$ extensions. Taken together, these results demonstrate the

13   efficacy of this functional screening platform for understanding myelination.

14

15   Keywords: Electrospinning, RNA interference, Non-viral Gene Delivery, Oligodendrocytes,

16   Oligodendrocyte Precursor Cells, microRNA

17

1 **1.   Introduction**

2   Oligodendrocytes (OLs), an important class of glia, are the myelinating cells of the central

3 nervous system (CNS). Myelination, the process by which OLs form multiple multilamellar sheaths

4 around axons, allows rapid sensory-motor coordination in vertebrates. As such, pathological loss of

5 myelin, or demyelination, impairs function due to disrupted action potential propagation as seen in

6 Multiple Sclerosis (MS) and spinal cord injuries (SCI).

7

8   Remyelination restores myelin sheaths to demyelinated axons to reinstate salutatory

9 conduction by following a sequence of events in a precise and temporally controlled fashion [1].

10 Following oligodendrocyte precursor cells (OPCs) activation and recruitment, OPCs differentiate into

11 OLs and ensheath axons (i.e. nascent myelin sheaths) before compacting into multilamellar myelin

12 sheaths (i.e. mature myelin wraps) [1-4]. However, these final stages of remyelination often fail to

13 transpire in MS and SCI [1]. The functional loss associated with failure in remyelination has

14 prompted the search for better therapeutics. Yet, the development of therapeutic strategies for

15 remyelination has been largely hindered by our lack of understanding of the intricate differentiation

16 and myelination processes. Hence, *in vitro* platforms that allow us both to study these processes and

17 at the same time enable functional screening of promising pro-myelinogenic therapeutics are highly

18 valuable [5].

19

20   Among the various stages that are involved in OPC differentiation, maturation and

21 myelination, the first two steps of differentiation and maturation of OPCs are often analyzed by

22 fairly straightforward immunohistochemical evaluations of specific OL markers such as CNPase,

23 Myelin Basic Protein (MBP) and others [6-9]. However, the main functionality of an OL is determined

24 at the final stage of myelination, where radial and longitudinal growths of myelin wraps occur [10].

3

1   Unfortunately, this final stage of myelination remains highly challenging to model in an *in vitro*

2   culture. Yet it is crucial to achieve robust aforementioned growth of myelin wraps to enable the

3   systematic examination of OL functionality and screening of therapeutics that can modulate

4   remyelination.

5

6   By mimicking the size scale and architecture of axons, electrospun fibers have been utilized

7   to replace neurons in conventional neuron-OL co-cultures for studies on myelination. This strategy

8   helps to remove influences of axonal signalling and reveals the intrinsic myelination capabilities of

9   OL in response to physical signals [11, 12]. While platforms comprising of dense electrospun fiber

10   mesh provide axon-mimicking physical cues to support OL myelination, it is difficult to do direct

11   imaging and quantification of the myelin [8, 9]. On the contrary, the sparse fiber platforms that were

12   engineered previously do not provide suspended fibers to prevent OPCs from sensing the stiff

13   underlying supporting substrate [13]. Moreover, the role of biochemical signalling is also crucial. Yet,

14   such a biofunctional axon-like substrate remains unavailable for probing the effects of potential

15   biochemical signals on myelination.

16

17   Here, we introduce a simple and versatile method to biofunctionalise microfiber scaffolds to

18   allow controlled and sustained delivery of promyelinogenic biomolecules to OPCs. This platform is

19   comprised of suspended-axon-mimicking fibers, which supports OL myelination. As compared to

20   conventional electrospun membranes, this platform also allows straightforward visualization of

21   myelination. We show that using the versatile mussel-inspired bioadhesive, polydopamine (PD),

22   coating, these axon-like fibers could be easily functionalized with drugs to serve as a reservoir for

23   sustained drug/gene delivery. Correspondingly, such scaffolds not only serve as potential drug/gene

24   screening platforms for identifying important promyelinogenic therapeutics but can also be easily

1 translated into direct implantable devices for future *in vivo* regeneration and remyelination purposes

2 [14].

3   As a proof-of-concept, we delivered a cocktail of microRNA (miR) mimics using this platform

4 to control, visualize and quantify OL differentiation and myelination. In particular, miR-219 and miR-

5 338 are potent post-transcriptional regulators that are involved in OPC development [15, 16]. We

6 previously showed that these miRs act synergistically to down-regulate the expression of inhibitors

7 of OPCs differentiation and promoted OPCs differentiation and maturation [8, 9]. More recently,

8 further evidence also suggests that the two miRs act in tandem to promote myelination [17]. Thus,

9 we hypothesized that PD fiber-mediated delivery of miR-219 and miR-338 will promote OPC

10 differentiation and myelination, which can be evaluated and quantified using our suspended

11 biofunctional, axon-mimicking microfiber platform.

12

13 **2.   Materials and Methods**

14 **2.1   Materials**

15   Polycaprolactone (PCL, Mw: 200,000) was purchased from PolySciTech. Polycaprolactone

16 (PCL, Mw: 45,000), 2,2,2-trifluoroethanol (TFE), dopamine hydrochloride, Dnase 1 type IV, Poly-D-

17 Lysine (PDL), N-Acetyl-L-Cysteine (NAC), D-biotin, ITS, Putrescine, L-Thyroxine (T4), Tri-iodothyronine

18 (T3), Progesterone, Bovine Serum Albumin (BSA), L-cysteine, Triton X-100 were purchased from

19 Sigma-Aldrich. Scramble negative control miR, miR-219, miR-338-3p, miR-338-5p mimics, Alexa-Fluor

20 488 goat anti-rat, Alexa-Fluor 633 goat anti-rabbit antibodies, minimum essential media (MEM),

21 DMEM High Glucose, Penicillin/Streptomycin (Pen/Strep) were purchased from Life Technologies.

22 NS21 supplement and Neuro Medium were purchased from Miltenyi Biotech. TransIT-TKO was

23 purchased from MirusBio. Rat anti-Myelin Basic Protein (MBP, aa82-87) was purchased from Bio-Rad.

1   Rabbit anti-Oligodendrocyte Transcription Factor 2 (Olig2, AB9610) was purchased from Merck.

2   Papain suspension was purchased from Worthington.

3

4   **2.2   Fabrication and characterisation of suspended microfiber substrate**

5   Figure 1A illustrates the engineering of the suspended microfiber platform. PCL pellets (MW:

6   45,000) were melted on a hot plate in a mould and allowed to cool and solidify into a block of PCL.

7   Following that, the block was embedded into optimal cutting temperature medium (OCT) and

8   cryosectioned into 20 μm films, which were then dried in a 37 ^{o}C oven. Two dried pieces of PCL films

9   were then placed at two opposing ends of a 15-mm diameter glass coverslip at a distance of 0.5 cm

10   apart and melted briefly on a hotplate at about 50 °C. These glass coverslips were then pasted onto

11   a rotating wheel with carbon tape. For electrospinning of microfibers, PCL (MW: 200,000) was

12   dissolved in TFE to make a 7 wt% solution. Thereafter, the homogeneous solution was loaded into a

13   syringe and dispensed at a fixed rate of 2 ml/h by a syringe pump (New Era pump system Inc., USA)

14   through a 22G needle. Positive 4 kV and -4 kV voltages (Gamma High Voltage, USA) were then

15   applied to the needle and rotating collector (730 rpm) respectively. The distance between the

16   needle and the collector was kept at 11.5 cm. After the fibers were collected, PCL films were melted

17   briefly again to allow the fibers to stick to the PCL films. Since the melted films may cause fibers to

18   slack and sink to the glass coverslips, to check if the fibers remained taut and suspended after the

19   process, we repeated the melting and collection processes 3 times. Thereafter, the dried suspended

20   microfiber scaffolds were secured by applying a layer of silicon glue around the circumference of

21   each coverslip.

22   For 3-dimensional (3D) imaging of myelin, di(thiophene-2-yl)-diketopyrrolopyrrole

23   conjugated PCL (PCL-DPP-PCL) fluorescent fibers were prepared according to previously reported

24   protocol [18]. Briefly, to ensure similar fiber diameter as plain PCL fibers, PCL was mixed with 1 wt%

1   of PCL-DPP-PCL in TFE to make a 12.5 wt% solution. Thereafter, the solution was dispensed at a flow

2   rate of 1.5 ml/h through a 21G needle for electrospinning. The collector was located 12 cm away and

3   rotated at 1500 rpm. Positive 12 kV and negative 4 kV voltages were applied on the needle and

4   collector respectively.

5

6   **2.3   Scanning electron microscopy**

7   The morphology of the microfibers was evaluated using scanning electron microscopy (SEM)

8   (JEOL, JSM-6390LA, Japan). Briefly, PCL substrates were attached onto the SEM support by carbon

9   tapes and sputter-coated with platinum for 60 s at 20 mA. Thereafter, the samples were imaged

10   under an accelerating voltage of 10 kV.

11

12   **2.4   Preparation of miR-loaded fibers**

13   The microfiber substrates were sterilised and wetted with 70% ethanol for 15 min. The

14   substrates were then incubated in 1 ml of 0.5 mg/ml dopamine hydrochloride solution for 4 h on an

15   orbital shaker to form the polydopamine (PD) coating. After 3 washes with DI water, the fibers were

16   further coated with 2 ml of 5 µg/ml PDL overnight and washed 3 times with DI water. For miR

17   adsorption, 2 µg of miR was complexed at 1:1 v/v ratio with the transfection reagent, TKO. The

18   amount of miR and its ratio with TKO have been optimised for high gene silencing and low cellular

19   toxicity based on our previous works [8, 9]. Specifically, 3 µl of 50 µM miR was complexed with 3 µl

20   of TKO for 15 min in 100 µl of DMEM. The complex was then added onto the PDL coated fibers and

21   incubated at 37 $^\circ$C for an hour. All substrates were divided into two groups: TKO with scrambled

22   Negative Control miR (NEG miR control); and TKO with equal masses of miR-219, miR-338-3p and

1   miR-338-5p (miR-219/miR-338). Substrates that were not used for the delivery of miRs were coated

2   with 5 µg/ml of PDL overnight and washed 3 times with DI water before cell seeding.

3

2.5   OPCs isolation and myelination culture

5   The isolation of primary OPCs from rats was approved by the Institutional Animal Care and

6   Use Committee (IACUC) at Nanyang Technological University, Singapore. The isolation and culture of

7   primary OPCs and the myelination culture were carried out according to two previously reported

8   protocols [12, 19]. Briefly, P0-P2 neonatal rat cortices that were cleaned from meninges were

9   enzymatically digested with 1.2 U Papain and 40 µg/ml DNase at 37 ^{o}C for 1 h. Thereafter, the

10   enzymatic activity was stopped with 8 ml of DMEM with 10% Fetal Bovine Serum (FBS) and the

11   dissociated tissues were triturated with a 21G needle and syringe. Tissues from 6 digested cortices

12   were seeded onto 4 PDL-coated T75 flasks and cultured in DMEM with 10% FBS and 1% Pen/Strep.

13   After 9-11 days, the OPCs were separated from the mixed glia culture by shaking on an orbital

14   shaker at 200 rpm for 1 h at 37 ^{o}C to remove the loosely attached microglia. This was followed by a

15   further 16-17 h of shaking. OPCs were then further purified by differential adhesion on untreated

16   petri dishes for 25 min. Through this isolation method, the purity of the OPCs attained was 95.3 ±

17   1.6 % (Supplementary Figure 1). Purified OPCs were then seeded at a density of 35,000 onto each

18   suspended fiber substrate, and cultured for 7 days in myelin medium, which consisted of

19   DMEM:Neurobasal (50:50), NS21, 1% Pen/Strep, Glutamax, ITS, 10 ng/ml biotin, 5 µg/ml NAC and

20   SATO (100 µg/ml BSA, 60 ng/ml Progesterone, 16 µg/ml Putrescine, 400 ng/ml T3 and T4).

21

2.6   Immunofluorescent staining

After 7 days, the cultures were fixed with 4% paraformaldehyde (PFA). The fixed myelin-fiber cultures were then permeabilised with 0.1% Triton-X for 15 min at room temperature. Next, the samples were incubated with primary antibodies overnight at 4 $^\circ$C, followed by secondary antibodies for 1 h at room temperature. The primary antibodies used were: rat anti-MBP (1:200) and rabbit anti-Olig2 (1:1000). The secondary antibodies used were: Alexa-Fluor 488 goat anti-rat and Alexa Fluor 633 goat anti-rabbit (both at 1:1000). The nuclei were counterstained with DAPI. The samples were then mounted onto 60 mm coverglass with Fluoromount-G and imaged under a Zeiss LSM 800 confocal microscope.

To calculate the percentage of MBP$^+$ cells with respect to DAPI (MBP$^+$/DAPI), 10 non-overlapping regions of interest (ROI) were chosen randomly for each substrate at 20x magnification. The percentages of MBP$^+$/DAPI were then calculated by (number of MBP$^+$ cells/number of DAPI) x 100% with an average of more than 140 DAPI$^+$ cells counted for each group per experiment. The percentages of MBP$^+$ cells with respect to OLIG2 (MBP$^+$/OLIG2$^+$) were computed by counting on an average of more than 110 OLIG2$^+$ cells from each group and using the formula: (number of MBP$^+$ cells/number of OLIG2$^+$ cells) x 100%. The experiment was repeated 3 times, resulting in the analysis of a total of more than 420 DAPI$^+$ and 330 OLIG2$^+$ cells per sample group.

To calculate the percentage of MBP$^+$ cells with myelin-like extensions/wrappings on fibers only, MBP$^+$ structures were thoroughly examined by looking at the entire z-layer (step size 0.75 µm) to observe any membrane formation on fibers and/or coverglass at 20x magnification. MBP$^+$ cells that formed membranes on fibers but not on cover glass were qualified as "MBP$^+$ cells with only myelin-like extensions on fibers". The percentage of MBP$^+$ cells with myelin-like extensions on fibers only was computed by (number of MBP$^+$ cells with only myelin-like extension on fibers only/total

1 number of MBP$^+$ cells) x 100%. On average more than 50 MBP$^+$ cells were evaluated from at least 10

2 ROI per substrate for each group. The experiment was repeated 3 times.

3

4   A myelin-like extension was defined as a continuous tube of MBP staining that stretched

5 along a fiber. To measure the length of myelin-like extensions on fibers, MBP signals from single

6 DAPI were traced along individual fibers at 40 x magnification. The measured lengths were then

7 plotted in logarithmic scale as "log(nascent sheath length)". Gaussian distribution was then used to

8 fit the distribution of log(nascent sheath length) for average length comparison [12]. On average 30

9 myelin-like wrappings were measured per experiment, resulting in a total of 196 nascent sheaths

10 being quantified in all 3 experimental repeats. To compute for the number of nascent myelin

11 sheaths per cell, 35 MBP$^+$ cells in the miR-219/miR-338 group and 30 MBP$^+$ cells in the negative miR

12 (NEG miR) group from 3 independent experiments were included in the analysis. All measurements

13 were done using the Fiji version of ImageJ [20].

14

15 **2.7   Statistical analysis**

16   All values were presented as mean ± standard error of mean (S.E.M). Student's t-test was

17 used to compare between NEG miR control and the miR-219/miR-338 group. P-values of less than

18 0.05 were considered to be statistically significant.

19

20 **3.   Results**

21 **3.1   Characterisation of suspended PCL microfiber substrates**

1   Figure 1A illustrates the engineered suspended-microfiber substrate. The average diameter

2   of the microfibers was 2.0 ± 0.3 μm, a diameter that is known to be permissive for myelination

3   (Figure 1B) [12, 13]. Supplementary Figure 2 shows that the fibers remained taut and suspended

4   even after 3 layers of PCL films were repeatedly melted and 3 layers of PCL fibers were deposited

5   after each melting.

6

7   Figure 1C shows that OPCs differentiated into MBP[+] OLs and appeared to ensheath the

8   microfiber substrates in the absence of miRs. Multiple MBP[+] extensions that were indicative of

9   nascent myelination were formed by OLs, as shown by the bright green MBP signals. These myelin-

10   like extensions ran along the electrospun fibers, as shown in Supplementary Figure 3. PCL-DPP-PCL

11   fibers fluoresce brightly at 568 nm wavelength upon excitation while green MBP signals ran in

12   conjunction. Supplementary Figure 3B shows a confocal 3D reconstruction view of an OL on the red

13   PCL-DPP-PCL fibers. Tubes of MBP signals were seen around red fibers, confirming MBP[+]

14   ensheathment of fibers by the OL. In the absence of growth factors, some OPCs underwent

15   apoptosis after 7 days in culture as indicated by the abnormally small and bright spots of DAPI

16   staining (Figure 1C). Concurrently, Olig2 expression was not detectable in these cells. Nonetheless,

17   the results suggest that this platform could support the formation of myelin-like extensions on the

18   suspended microfibers.

19

20   **3.2   Scaffold-mediated miR-219 / miR-338 delivery promoted OPC differentiation in the**

21   **absence of mitogen**

22   OPCs remained viable and differentiated into MBP[+] OLs on PD-PDL coated substrates after

23   transfection with miRs. Figure 2A shows that purified OPCs differentiated into OLIG2 and MBP

24   expressing OLs on the miR-adsorbed platforms. In particular, a higher percentage of MBP[+] OLs was

seen with miR-219 and miR-338 treatment. Thus, miR cocktail promoted OPC differentiation in a pro-differentiation, mitogen-free environment. Specifically, a 1.42-fold and 1.40-fold increase in the percentage of MBP$^+$ cells were observed when normalized against DAPI and OLIG2 respectively, when the OPCs were transfected with 2 μg of miR cocktail ($p < 0.05$, Figure 2B and Figure 2C). The results show that miR-219 and miR-338 acted in synergy with the myelination medium and further promoted the differentiation and maturation of OPCs.

3.3   Scaffold-mediated miR-219 / miR-338 delivery promoted the formation of myelin-like extensions on fiber

In our platform, PCL fibers were suspended at a distance of about 20 μm above the glass coverslip surface using PCL films. The low fiber density allowed OPCs to pass through the gaps between electrospun fibers and adhere to the coverslip while maintaining contact with the suspended fibers. As OPCs were in contact with both 2D and 3D substrates, they were able to form both flat membranes on the cover-glass and myelin processes that tracked along or partially covered the fibers as they differentiated into OLs (Figure 3A).

As shown in Figure 3B, OLs preferred to form MBP$^+$ extensions or nascent myelin sheaths along the axon-mimicking fibers when they were treated with the cocktail of miRs. Specifically, miR-219 / miR-338 treatment induced 2.9-fold more MBP$^+$ cells forming only myelin-like wrappings on fibers ($p < 0.01$, Figure 3C). On the other hand, OLs that were subjected to Neg miR treatment (Control group) had an inclination towards forming both MBP$^+$ extensions or nascent myelin sheaths on fibers and myelin membranes on coverglass, or myelin membranes only (Figure 3A). Thus, miR-219 / miR-338 enhanced the interaction of OPCs with 3D axon-like substrates, suggesting that biomolecules could alter cellular response towards physical cues.

1

3.4   Scaffold-mediated miR-219 / miR-338 delivery promoted longer fiber ensheathment

Substrate-mediated delivery of miRs increased the length of fiber ensheathment by OLs on the substrates (Figure 4 and Supplementary Figure 4). In the presence of miR-219 and miR-338, OLs formed significantly longer nascent myelin sheaths around the suspended fibers (Figure 4A and Supplementary Figure 4A for miR-219 / miR-338, Supplementary Figure 4B for NEG miR). Quantification results as illustrated in Figure 4B shows that the distribution of the length of fiber ensheathment shifted towards a larger value when the cells were treated with the miR cocktail. Specifically, 1.94-fold longer nascent myelin sheaths were formed by the OLs when they were treated with the cocktail of miR-219 / miR-338 (Figure 4C).

3.5   Scaffold-mediated miR-219 / miR-338 delivery promoted the formation of more myelin-like extensions per cell

OLs formed multiple myelin-like extensions along multiple fibers on the substrates. This attribute of OLs was altered by substrate-mediated delivery of miRs. In particular, miR-219 and miR-338-treated OLs had a higher number of myelin-like extensions being formed by each cell (Figure 5A). Specifically, miR-219 and miR-338-treated group had on average of 8.69 myelin extensions per OL as compared to 4.77 in the NEG miR treated group ($p < 0.01$, Figure 5B). Thus, both sheath number and length that were formed by individual OLs were enhanced on this substrate by substrate-mediated non-viral delivery of miR-219 / miR-338.

4.   Discussion

1   OLs are known to not require dynamic axonal signalling to initiate myelination [21]. Hence,

2   microfibers, micropillars and microbeads have been engineered to uncouple the axon-OL crosstalk

3   and provide biophysical cues for myelination studies [5, 11, 22]. While bolus supplementation of

4   biomolecules could provide the necessary biochemical signals for cells on the aforementioned

5   substrates, integrating biomolecules into tissue-engineered scaffolds could better recapitulate the *in*

6   *vivo* microenvironment, which is known to impact OLs behaviour [23]. Thus, we developed a surface-

7   functionalized platform to evaluate myelination using mussel-inspired PD coating.

8

9   OL differentiation and myelination are two different stages of OPC development with

10   distinctive mechanisms [24]. In our previous work, our fiber mesh-mediated miR delivery platform

11   promoted the differentiation and maturation of NG2$^+$ OPCs into RIP$^+$ and MBP$^+$ cells with high

12   viability [8, 9]. However, robust myelination *in vitro* requires optimisation of culture conditions and

13   scaffold design for optimal biochemical and physical signaling. Moreover, the new platform should

14   enable simple visualization, imaging and quantification of the extent of myelination. Thus, we

15   engineered a low fiber density, axon-mimicking drug delivery model, specifically for these purposes.

16   A low fiber density platform allows straightforward confocal imaging and quantification of myelin.

17   With this, we were able to demonstrate physiologically-relevant myelin membrane extension by

18   amalgamating physical cues from the low-density microfibers and biochemical signalling from the

19   miR-219 / miR-338 cocktail (Figure 1, 4-5).

20

21   PD-coated suspended microfiber substrates enabled effective surface adsorption of miRs

22   without altering the topography of the electrospun fibers. These miRs could then be released in a

23   sustained fashion and provide surface-mediated signalling, as shown in our previous studies [8, 9, 25,

24   26]. Conventional siRNA or miRNA studies employ bolus transfection, where cells are exposed to

1   RNAs transiently. However, sustained delivery of RNA complexes can have significantly better gene

2   silencing efficiency than bolus transfection, which can be translated to more efficient OPC

3   differentiation and maturation [9]. Furthermore, surface-adsorbed RNAs that were not released

4   could be directly internalised by OPCs [26]. This mimics axon-OL biochemical signalling and further

5   asserts the physiological relevance of our platform. All in all, we showed that substrate-mediated

6   miR delivery enhanced OPC differentiation and membrane extension on our platform (Figure 2-5).

7   Moreover, we have previously employed similar electrospun substrates for the delivery of proteins

8   and low molecular weight drugs [27-29]. Thus, this microfiber substrate could be a versatile

9   functional drug/gene screening platform for OLs.

10

11   In our previous study, we employed a similar platform to knock down RE-1 Silencing

12   Transcription Factor (REST) in mesenchymal stem cells (MSCs) using siRNA to enhance neuronal

13   differentiation [25]. While we observed pro-neuronal differentiation effect of siREST when MSCs

14   were subjected to conditions that were non-specific and suboptimal for such differentiation, the

15   advantage of siREST was not seen when optimal neuronal differentiation condition was employed

16   [25]. The results suggested that the gene silencing of REST was effective only in non-specific

17   differentiation conditions. In contrast, miR-219 and miR-338 appeared to act in synergy with pro-

18   myelinogenic culture conditions. miR-219 and miR-338 have been elucidated to be the key miRs that

19   are involved in OL maturation. These two miRs suppress critical inhibitory genes of OPC

20   differentiation and myelination (PDGFRα, Sox6, FoxJ3, ZFP238) or inhibitory signalling pathways

21   (NOTCH, LINGO) [6, 17]. Specifically, platelet-derived growth factor (PDGF) and fibroblast growth

22   factor (FGF) are well known mitogenic factors. Their removal from culture medium results in the

23   rapid differentiation of OPCs into OLs *in vitro*. All previous *in vitro* experiments that analyzed the

24   efficacy of miR-219 and miR-338 on directing OL differentiation utilized PDGF and FGF supplemented

25   culture media [6, 8, 9]. Under such proliferative conditions, miR-219 / miR-338 promoted OPC

1   differentiation into MBP$^+$ OLs. In contrast, we employed myelin-promoting medium in this study,

2   which comprised of a defined medium with no OPC mitogenic factors. Correspondingly, we showed

3   for the first time that miR-219 and miR-338 could significantly promote OPC differentiation into

4   mature MBP$^+$ OLs, even in such mitogen-free, pro-differentiation environment (Figure 2). This

5   suggests that miR-219 and miR-338 are potent factors in controlling OPC cell fate.

6

7   OPCs cultured on 2-dimensional (2D) glass coverslips or culture dishes form flat myelin

8   membrane sheets on the glass or plastic surface as they differentiate and mature into OLs [30]. On

9   the other hand, OLs cultured on suspended fibers formed only myelin-like wrappings around the

10   fibers [12]. In our platform, we observed an interesting phenomenon where scaffold-mediated

11   delivery of miR-219 and miR-338 promoted the formation of only MBP$^+$ extensions on fibers (Figure

12   3). The inclination to form structures that are indicative of myelin sheaths by wrapping around the

13   fibers rather than spreading membranes on the glass surface could be a pro-myelination indicator.

14   Future studies could elucidate the mechanistic differences between flat myelin membrane and

15   myelin sheath formation by OLs under the influence of miR-219/miR-338. In addition, ultrastructural

16   analyses using transmission electron microscopy could also provide useful insights into the effects of

17   miR-219/miR-338 on the integrity and structure of the formed myelin.

18

19   Although *in vitro* CNS myelin sheath length is an intrinsic property of OL [12], this

20   "myelinogenic potential" [31] of OL can be influenced by the underlying substrates. Firstly,

21   substrates can alter this potential by activating signalling molecules through a surface receptor.

22   Specifically, coating fiber substrates with laminin to reconstruct physiological OL-ECM interactions

23   promoted the formation of significantly more myelin sheaths per OL [12]. In this work, we presented

24   distinctive mechanism on how substrates could also be employed to deliver molecules into

1 OPCs/OLs and remodel their myelinogenic potential. Specifically, our substrate-mediated delivery of

2 miR-219 and miR-338 changed how OLs spread their membranes on glass or fibers (Figure 3-5). The

3 diverse mechanisms underlined the versatility of electrospun substrates in controlling myelination

4 and reinforced the notion that our microfiber-substrate could serve as an effective functional testing

5 platform for OL myelination.

6

7 Apart from serving as an *in vitro* platform for understanding myelination, electrospun fibers

8 may also be designed into directly implantable substrates for *in vivo* nerve regeneration applications,

9 such as in the case of spinal cord injury treatment [14]. In particular, the biomimicking topography of

10 electrospun fibers provides contact guidance to nerve regeneration while the sustained delivery of

11 drugs and genes from these scaffolds offers synergistic biochemical signaling to direct cell fate and

12 tissue regrowth [14]. Thus, promising drugs or genes as assessed on these fiber platforms may be

13 directly translated to *in vivo* testing. This avoids the need to redesign a new implantable platform

14 that carries the promising drug/gene; hence speeding up the process of drug development.

15

16 **5.   Conclusion**

17 In the present study, we developed a microfiber platform for *in vitro* myelination study and

18 functional screening of drugs/genes. Using miR-219 and miR-338 as the model drugs, we showed

19 that these miRs promoted OPC differentiation on our microfiber constructs. Moreover, we also

20 showed that the miRs promoted the ensheathment of fibers instead of the formation of flat myelin

21 membranes. OLs transfected non-virally with miRs also possessed longer nascent myelin sheaths and

22 more MBP$^+$ extensions per cell. This platform could be employed for further drug/gene testing and

23 translation into *in vivo* remyelination scaffold design.

References

[1] Franklin RJ, Ffrench-Constant C. Remyelination in the CNS: from biology to therapy. Nat Rev Neurosci 2008;9:839-55.

[2] Armstrong RC, Le TQ, Frost EE, Borke RC, Vana AC. Absence of fibroblast growth factor 2 promotes oligodendroglial repopulation of demyelinated white matter. The Journal of Neuroscience 2002;22:8574-85.

[3] Chari DM, Blakemore WF. Efficient recolonisation of progenitor-depleted areas of the CNS by adult oligodendrocyte progenitor cells. Glia 2002;37:307-13.

[4] Franklin RJ, Gilson JM, Blakemore WF. Local recruitment of remyelinating cells in the repair of demyelination in the central nervous system. Journal Of Neuroscience Research 1997;50:337-44.

[5] Mei F, Fancy SP, Shen YA, Niu J, Zhao C, Presley B, Miao E, Lee S, Mayoral SR, Redmond SA, Etxeberria A, Xiao L, Franklin RJ, Green A, Hauser SL, Chan JR. Micropillar arrays as a high-throughput screening platform for therapeutics in multiple sclerosis. Nat Med 2014;20:954-60.

[6] Zhao X, He X, Han X, Yu Y, Ye F, Chen Y, Hoang T, Xu X, Mi QS, Xin M, Wang F, Appel B, Lu QR. MicroRNA-mediated control of oligodendrocyte differentiation. Neuron 2010;65:612-26.

[7] Miron VE, Boyd A, Zhao JW, Yuen TJ, Ruckh JM, Shadrach JL, van Wijngaarden P, Wagers AJ, Williams A, Franklin RJ, ffrench-Constant C. M2 microglia and macrophages drive oligodendrocyte differentiation during CNS remyelination. Nat Neurosci 2013;16:1211-8.

[8] Diao HJ, Low WC, Lu QR, Chew SY. Topographical effects on fiber-mediated microRNA delivery to control oligodendroglial precursor cells development. Biomaterials 2015;70:105-14.

[9] Diao HJ, Low WC, Milbreta U, Lu QR, Chew SY. Nanofiber-mediated microRNA delivery to enhance differentiation and maturation of oligodendroglial precursor cells. J Control Release 2015;208:85-92.

[10] Chang KJ, Redmond SA, Chan JR. Remodeling myelination: implications for mechanisms of neural plasticity. Nat Neurosci 2016;19:190-7.

[11] Lee S, Leach MK, Redmond SA, Chong SY, Mellon SH, Tuck SJ, Feng ZQ, Corey JM, Chan JR. A culture system to study oligodendrocyte myelination processes using engineered nanofibers. Nat Methods 2012;9:917-22.

[12] Bechler ME, Byrne L, Ffrench-Constant C. CNS Myelin Sheath Lengths Are an Intrinsic Property of Oligodendrocytes. Curr Biol 2015;25:2411-6.

[13] Lee S, Chong SYC, Tuck SJ, Corey JM, Chan JR. A rapid and reproducible assay for modeling myelination by oligodendrocytes using engineered nanofibers. Nature Protocols 2013;8:771-82.

[14] Nguyen LH, Gao M, Lin J, Wu W, Wang J, Chew SY. Three-dimensional aligned nanofibers-hydrogel scaffold for controlled non-viral drug/gene delivery to direct axon regeneration in spinal cord injury treatment. Sci Rep 2017;7:42212.

[15] Emery B. Transcriptional and post-transcriptional control of CNS myelination. Current Opinion in Neurobiology 2010;20:601-7.

[16] He X, Yu Y, Awatramani R, Lu QR. Unwrapping myelination by microRNAs. Neuroscientist 2012;18:45-55.

[17] Wang HB, Moyano AL, Ma ZY, Deng YQ, Lin YF, Zhao CT, Zhang LG, Jiang MQ, He XL, Ma ZX, Lu FH, Xin M, Zhou WH, Yoon SO, Bongarzone ER, Lu QR. miR-219 Cooperates with miR-338 in Myelination and Promotes Myelin Repair in the CNS. Developmental Cell 2017;40:566-+.

[18] Diao HJ, Wang K, Long HY, Wang M, Chew SY. Highly Fluorescent and Photostable Polymeric Nanofibers as Scaffolds for Cell Interfacing and Long-Term Tracking. Adv Healthc Mater 2016;5:529-33.

[19] Chen Y, Balasubramaniyan V, Peng J, Hurlock EC, Tallquist M, Li J, Lu QR. Isolation and culture of rat and mouse oligodendrocyte precursor cells. Nat Protoc 2007;2:1044-51.

[20] Schindelin J, Arganda-Carreras I, Frise E, Kaynig V, Longair M, Pietzsch T, Preibisch S, Rueden C, Saalfeld S, Schmid B, Tinevez JY, White DJ, Hartenstein V, Eliceiri K, Tomancak P, Cardona A. Fiji: an open-source platform for biological-image analysis. Nature Methods 2012;9:676-82.

[21] Rosenberg SS, Kelland EE, Tokar E, De La Torre AR, Chan JR. The geometric and spatial constraints of the microenvironment induce oligodendrocyte differentiation. Proceedings of the National Academy of Sciences 2008;105:14662-7.

[22] Redmond SA, Mei F, Eshed-Eisenbach Y, Osso LA, Leshkowitz D, Shen YA, Kay JN, Aurrand-Lions M, Lyons DA, Peles E, Chan JR. Somatodendritic Expression of JAM2 Inhibits Oligodendrocyte Myelination. Neuron 2016;91:824-36.

[23] Rosenberg SS, Kelland EE, Tokar E, De la Torre AR, Chan JR. The geometric and spatial constraints of the microenvironment induce oligodendrocyte differentiation. Proc Natl Acad Sci U S A 2008;105:14662-7.

[24] Emery B. Regulation of Oligodendrocyte Differentiation and Myelination. Science 2010;330:779-82.

[25] Low WC, Rujitanaroj PO, Lee DK, Kuang J, Messersmith PB, Chan JK, Chew SY. Mussel-Inspired Modification of Nanofibers for REST siRNA Delivery: Understanding the Effects of Gene-Silencing and Substrate Topography on Human Mesenchymal Stem Cell Neuronal Commitment. Macromol Biosci 2015;15:1457-68.

[26] Low WC, Rujitanaroj PO, Lee DK, Messersmith PB, Stanton LW, Goh E, Chew SY. Nanofibrous scaffold-mediated REST knockdown to enhance neuronal differentiation of stem cells. Biomaterials 2013;34:3581-90.

[27] Handarmin, Tan GJY, Sundaray B, Marcy GT, Goh ELK, Chew SY. Nanofibrous scaffold with incorporated protein gradient for directing neurite outgrowth. Drug Delivery and Translational Research 2011;1:147-60.

[28] Liu T, Xu JY, Chan BP, Chew SY. Sustained release of neurotrophin-3 and chondroitinase ABC from electrospun collagen nanofiber scaffold for spinal cord injury repair. Journal of Biomedical Materials Research Part A 2012;100A:236-42.

[29] Low WC, Rujitanaroj PO, Wang F, Wang J, Chew SY. Nanofiber-mediated release of retinoic acid and brain-derived neurotrophic factor for enhanced neuronal differentiation of neural progenitor cells. Drug Delivery and Translational Research 2015;5:89-100.

[30] Zuchero JB, Fu MM, Sloan SA, Ibrahim A, Olson A, Zaremba A, Dugas JC, Wienbar S, Caprariello AV, Kantor C, Leonoudakis D, Lariosa-Willingham K, Kronenberg G, Gertz K, Soderling SH, Miller RH, Barres BA. CNS myelin wrapping is driven by actin disassembly. Dev Cell 2015;34:152-67.

[31] Chong SYC, Rosenberg SS, Fancy SPJ, Zhao C, Shen Y-AA, Hahn AT, McGee AW, Xu X, Zheng B, Zhang LI, Rowitch DH, Franklin RJM, Lu QR, Chan JR. Neurite outgrowth inhibitor Nogo-A establishes spatial segregation and extent of oligodendrocyte myelination. Proceedings of the National Academy of Sciences 2012;109:1299-304.

Figure Captions

Figure 1: Electrospun microfiber platform for OL functional drug testing. (A) Workflow of suspended microfiber substrate. (B) SEM image showed that electrospun microfiber has diameter of 2.0 ± 0.3 μm (100 fibers were measured). (C) OPCs differentiated into OL and extended myelin-like MBP$^+$ structures along the suspended fibers as shown by lines of green MBP signals.

Figure 2: Scaffold-mediated delivery of miR-219/miR-338 promoted OPCs differentiation in the absence of mitogen. (A) Representative confocal images show that cocktail of miRs promoted differentiation of OPCs into MBP$^+$ OL. (B) Quantitative data shows miR-219 and miR-338 treatment resulted in more MBP$^+$ cells per DAPI. (C) Quantitative data shows miR-219 and miR-338 treatment resulted in more MBP$^+$ cells per OLIG2$^+$ cell. $^\#$ indicates $p < 0.05$; two-tailed t test, with an average of more than 140 DAPI and 110 OLIG2$^+$ cells quantified from each experimental group per experiment (n=3).

Figure 3: Scaffold-mediated delivery of miR-219/miR-338 promoted formation of MBP$^+$ myelin-like extensions on fiber instead of membrane on glass coverslip. (A) Confocal images showing formation of both myelin-like extensions on fiber and myelin membrane on coverglass by the same cell. (B) Representative confocal images show miR-219/miR-338 promoted formation of myelin-like wrappings around fibers. (C) Quantitative data shows miR-219 and miR-338 treatment allowed higher percentage of MBP$^+$ cells to form myelin-like extensions only. * indicate $p < 0.01$; two-tailed t test, with at least 50 MBP$^+$ cells from each group per experiment (n = 3).

Figure 4: Scaffold-mediated delivery of miR-219/miR-338 increased myelin-like extension length of OL. (A) Representative confocal images show miR-219 and miR-338 treatment resulted in longer myelin-like extension length on suspended fiber platform. (B) Frequency distribution shows a shift of extension length distribution towards higher values when OPCs were treated with miR-219 and miR-338. (C) Log transformation of lengths shows distribution of length of myelin-like extensions, with significant difference between the mean of miR-219/miR-338 and NEG miR treated group. * indicate $p < 0.01$; two-tailed t test, 196 extensions measured from 3 independent experiments.

Figure 5: Scaffold-mediated delivery of miR cocktail increased number of myelin-like extensions per OL. (A) Representative confocal images show miR-219/miR-338 enhanced formation of more myelin-like extensions per OL. (B) Distribution of number of myelin-like extension per OL. Quantitative data shows miR-219/miR-338 treatment resulted in higher average number of myelin-like extensions per OL. Each dot represents one cell * indicate $p < 0.01$; two-tailed t test, 35 cells in miR-219/miR-338 group and 30 cells in NEG miR group, from 3 independent experiments.

Supplementary figure 1: Confocal images show more than 95% pure OPCs following isolation.

Supplementary figure 2: SEM images of cross section of microfiber substrate. With repeated melting of PCL film and repeated fiber deposition, suspended fibers remained taut in layers. (A) Low magnification view shows fibers suspended in layers above glass coverslip. (B) Higher magnification view shows taut fibers.

Supplementary figure 3: MBP$^+$ wrapping on fluorescent PCL-DPP-PCL fibers. (A) Confocal image shows MBP signals ran along red coloured fibers. (B) 3D-reconstruction image shows MBP$^+$ tubular structures surrounding red fluorescent PCL-DPP-PCL fibers. (C) 95.3 ± 1.6 % of the cells expressed OPCs NG2 marker 1 day post seeding.

Supplementary figure 4: Video across different z-stack layers showing MBP$^+$ extensions running along the fibers on both miR-219/miR-338 and NEG miR treated OPCs.

A — PCL film → Coverglass; Electrospinning; Thin Suspended PCL fiber

B — 10 µm

C — DAPI | OLIG2 | MBP | Merged | 10 µm
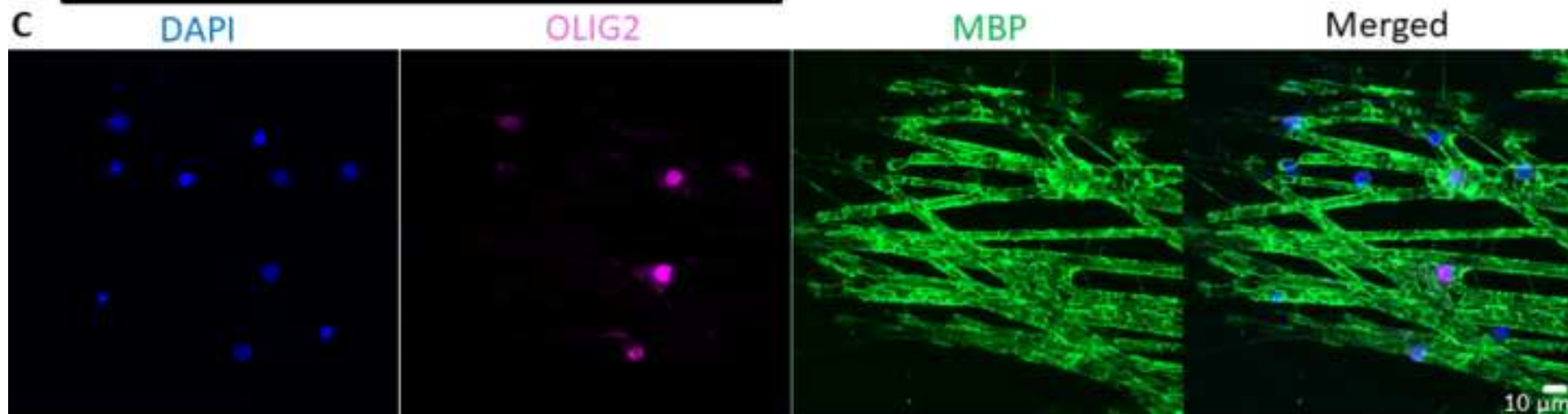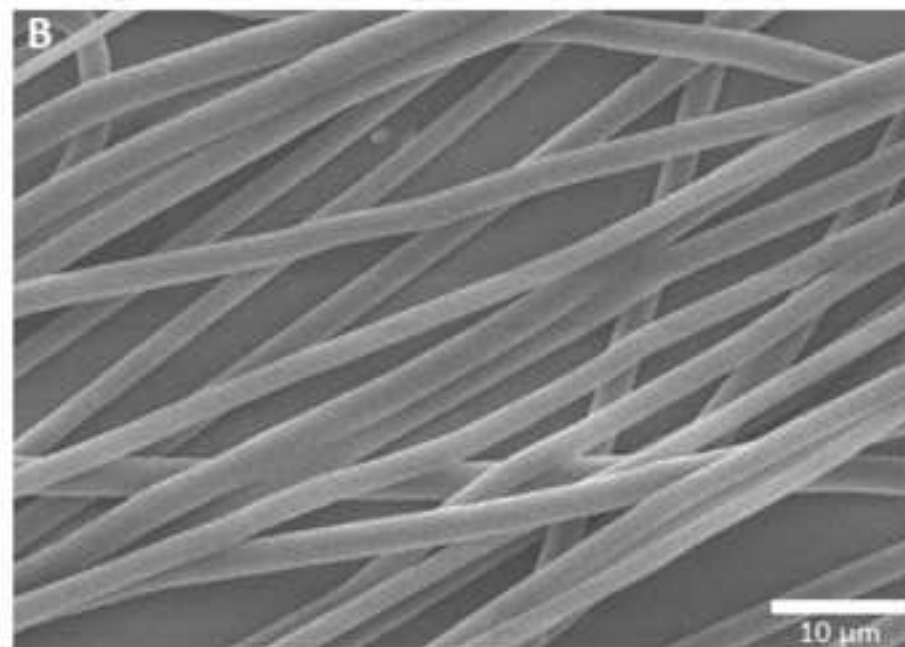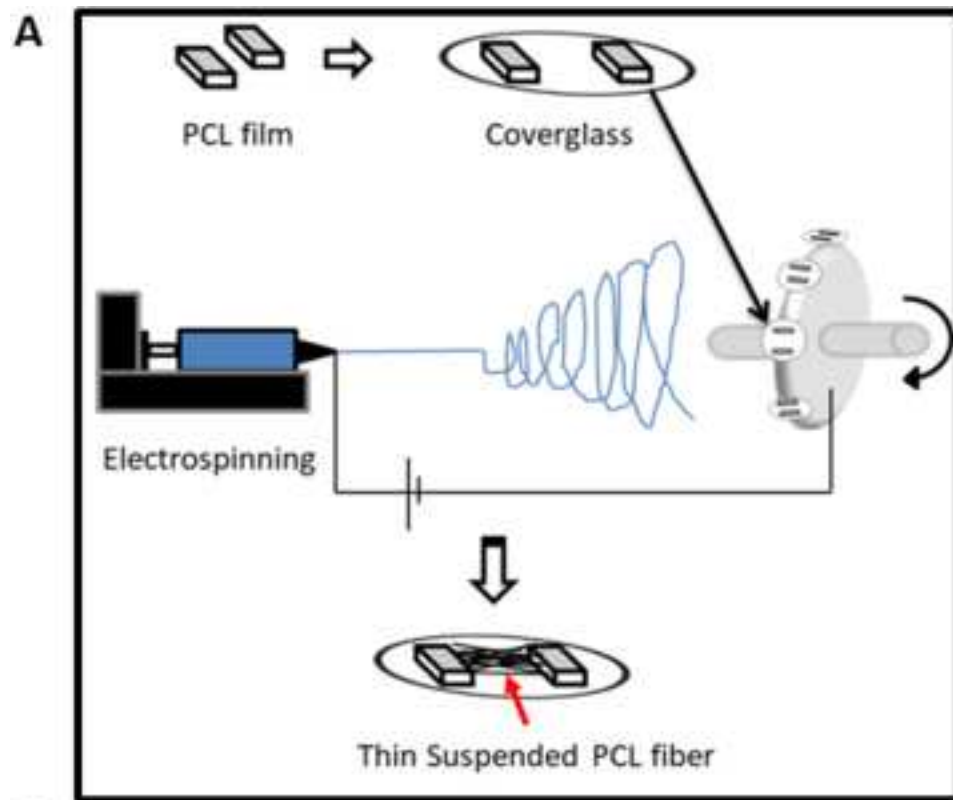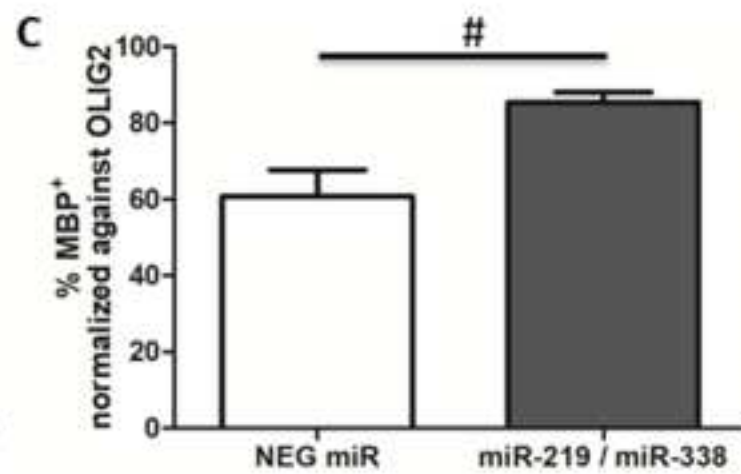
Figure 2

Figure 3
Click here to download high resolution image
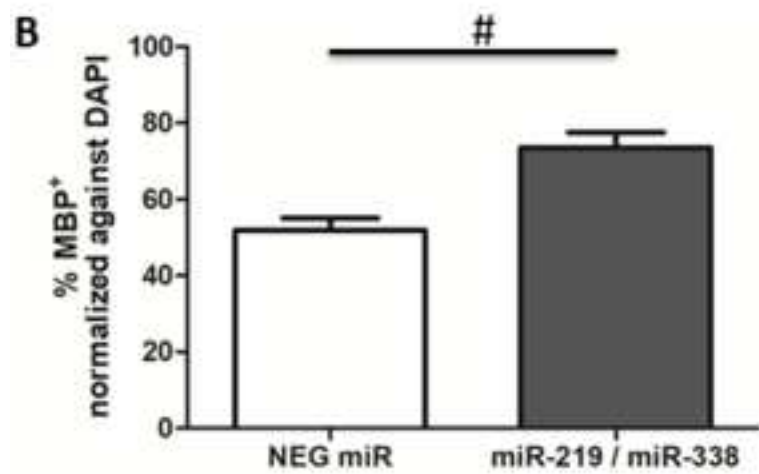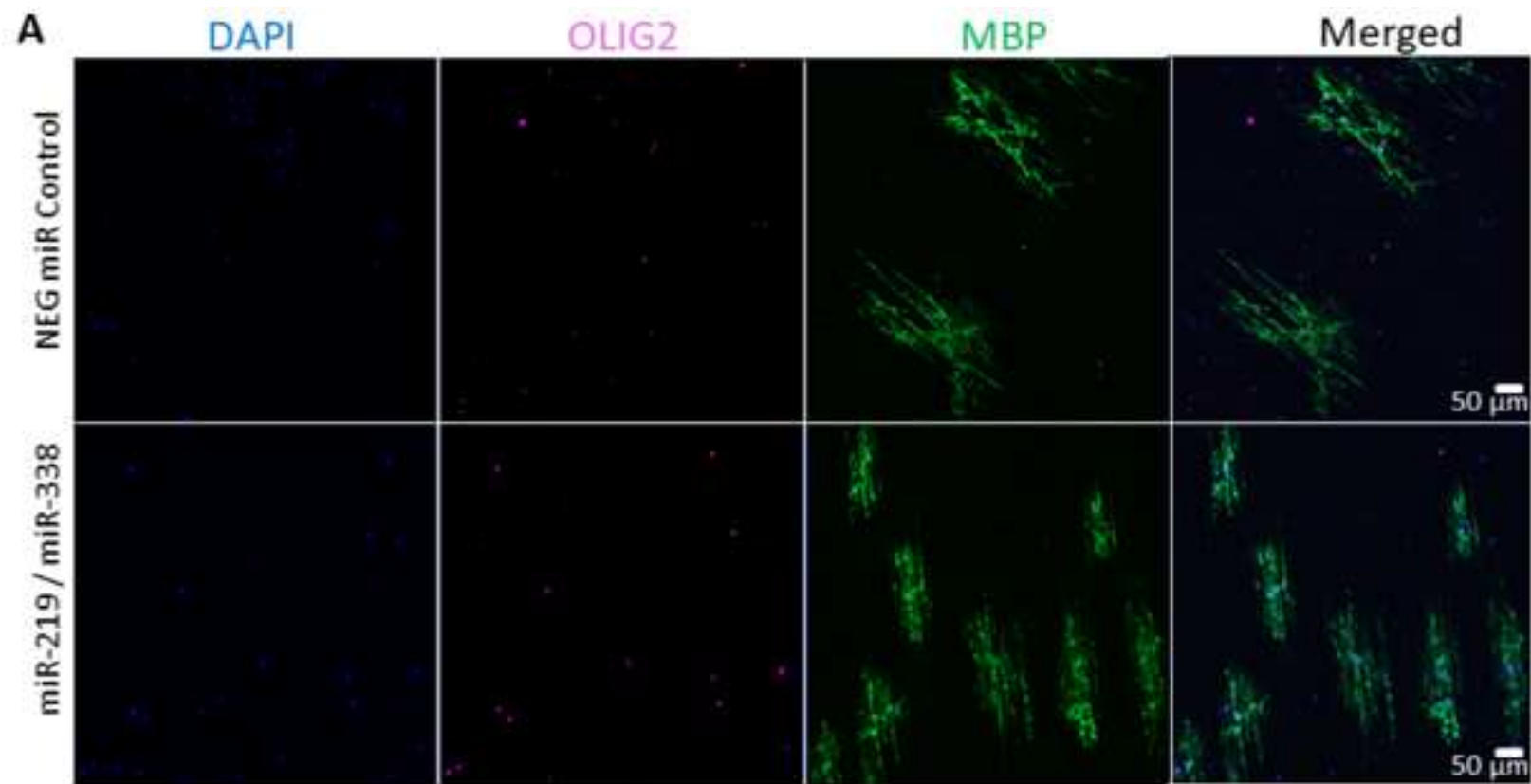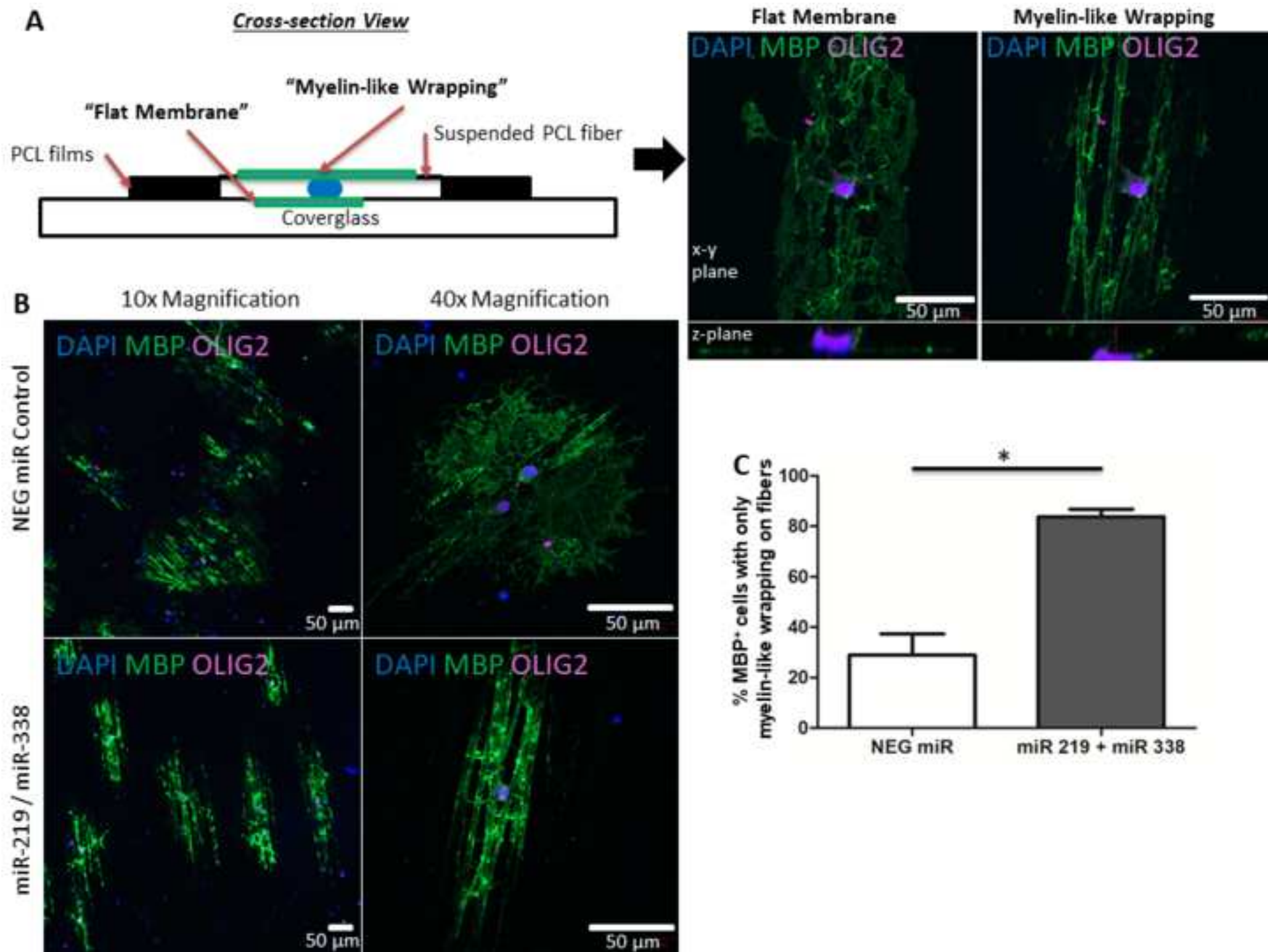
Figure 4
[Click here to download high resolution image](#)
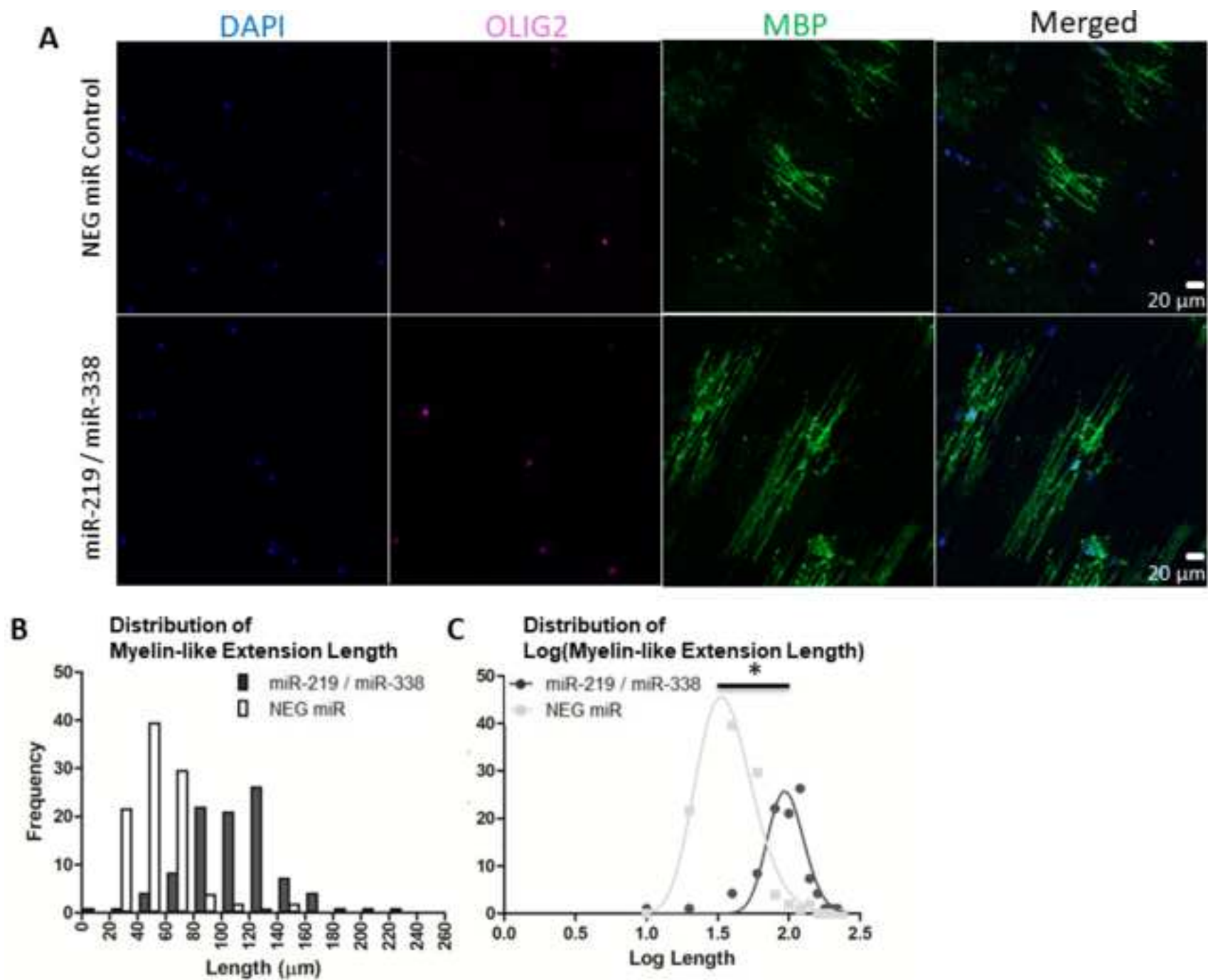
Figure 4

Figure 5
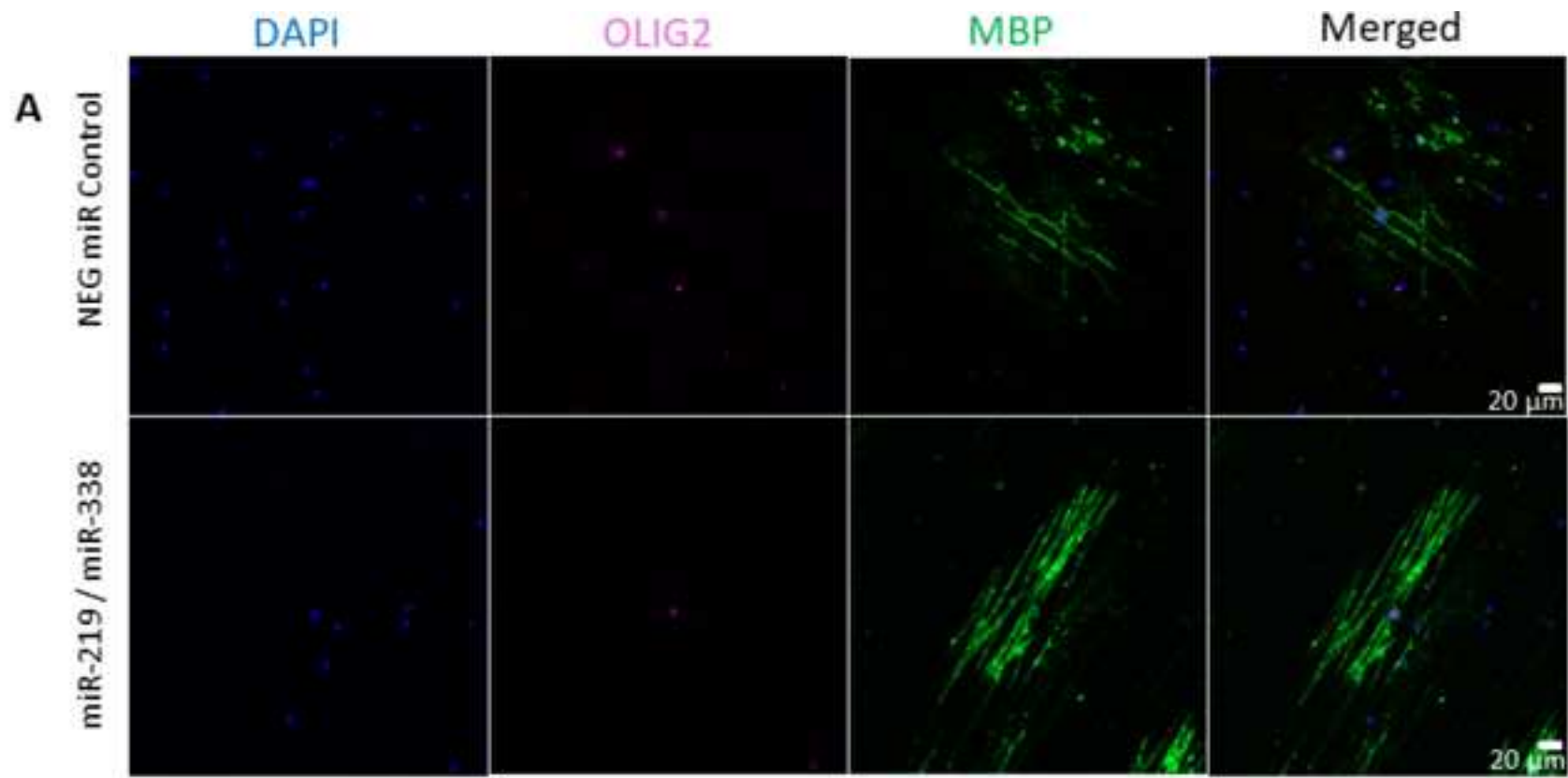[Click here to download high resolution image](#)

Figure 5

A

	DAPI	OLIG2	MBP	Merged
NEG miR Control				20 μm
miR-219 / miR-338				20 μm

B

Scatter plot: Number of Extension per OL (y-axis, 0 to 20) for NEG miR and miR-219 / miR-338. A significance marker (*) is shown above, comparing the two groups. NEG miR shows values clustered around 5, while miR-219 / miR-338 shows values clustered around 9.

Supplementary Figure 1

Supplementary Figure 2

Supplementary Figure 3

Supplementary Figure 4A

Supplementary Figure 4B